The temperature dependence for the third shell's Fourier-peak of Nb-EXAFS in $KNbO_3$ as additional source of information on the local atomic structure

Lusegen A. Bugaev, Victoria A. Shuvaeva Konstantin N. Zhuchkov, Elizaveta B. Rusakova, and Rostislav V. Vedrinskii

Department of Physics, Rostov University, Zorge str., 5, Rostov-on-Don, 344090, RUSSIA
E-mail: bugaev@rnd.runnet.ru

The information on the structure of tetragonal $KNbO_3$ is extracted from the temperature dependence of the third shell's Fourier-peak of Nb-EXAFS. It is shown that this dependence can be explained by two effects: 1) rigid rotations of the O_6-octahedron and 2) increase of the third shell's DW–parameter. However, diffraction data on the temperature dependence of the DW-parameter permit us to conclude that the last effect only is sufficient and the O_6-octahedron rotation doesn't occur in the high-temperature phases of $KNbO_3$. Using EXAFS it is revealed that in the neighboring cells Nb-atoms are parallel shifted closely to [211] direction in tetragonal phase.

Keywords: EXAFS; local atomic structure; ferroelectrics; $KNbO_3$.

1. Introduction

The temperature dependencies of EXAFS-spectra for ABO_3 crystals have been studied and used extensively (Bell et al., 1991; Petit P.E. et al., 1997; Sicron N. et al., 1997) to determine the local structure distortions. In previous papers (Bugaev et al., 1997; Bugaev et al., 1999) the approach for identifying the B-atoms displacements from the ideal positions in perovskite type ABO_3 crystals using EXAFS, measured under different temperatures, was proposed. The approach is based on the observed qualitative differences in the imaginary parts (Im F(r)) of EXAFS Fourier-transforms (FT) for different models of atomic displacements within the first shell (O_6-octahedron) r-range. The analysis of F(r) for experimental Nb-EXAFS in $KNbO_3$ in a wide temperature region was performed (Bugaev et al., 1998; Bugaev et al., 1999) using the results of calculations for the first shell contribution to $\chi(k)$ obtained for alternative models of structural distortions from the ideal perovskite. These models were generated using the diffraction data on the fixed value of Nb displacement projection on the polar axis in the studied phase of $KNbO_3$. Using this approach, the directions and the corresponding values of Nb displacements from the centers of O_6-octahedra in high-temperature phases of $KNbO_3$ were obtained. However the analysis of the first shell term $\chi_1(k)$ provides the only information on the B-atoms positions relatively to the nearest oxygen atoms and therefore is insufficient to solve the problems of B-atoms displacements in the neighboring cells, the rotation and the rigidity of the O_6-octahedron, etc. To overcome these limitations and to obtain additional structural information, in the present paper the F(r) behavior within the third shell (B-atoms) r-region is studied consistently with the results obtained earlier (Bugaev et al., 1997; Bugaev et al., 1998; Bugaev et al., 1999) from the analysis of the first shell contribution. In ABO_3 crystals the third shell is usually well distinguished in |F(r)| of B-atom's EXAFS due to the photoelectron multiple-scattering (MS) processes on B(abs.atom) – O(first shell) – B(third shell) atomic chains. This focusing effect and the corresponding third shell's peak value in $|F(r)|$ rapidly decreases with the increase of $\Delta\left(\overline{BO},\overline{OB}\right)$ –bond angle in B-O-B chain, which permits to obtain the structure information on the O_6-octahedron behavior under the changed experimental conditions such as the applied temperatures, pressures or electric fields.

2. EXAFS simulations

The experimental temperature dependence of the third shell's peak value in |F(r)| of Nb-EXAFS in $KNbO_3$ is presented in Fig.1. The observed decrease of the third shell's (Nb-atoms) peak with the temperature is accompanied by the stable frequency of Im F(r) oscillations and therefore such a behavior is usually explained by the temperature increase of the Debye-Waller (DW) parameter σ^2. To distinguish this effect and the O_6-octahedron rotation, which often occur in ABO_3, on the third shell's peak value, we have simulated this rotation through the Nb-O-Nb chain, moving the O-atom by d from the Nb-Nb direction. The third shell's term $\chi_3(k)$ was calculated with the different values of oxygen displacements d=0.0, 0.1, 0.2, 0.3, 0.5 Å and the corresponding |F(r)| and Im F(r), obtained within the k-range from k_{min}=3.8 $Å^{-1}$ to k_{max}=15.5 $Å^{-1}$ are presented in Fig.2. As can be seen the simulation of the O_6–octahedron rotation is reflected in the decrease of the Nb (third shell) peak in |F(r)| under the stable frequency of oscillation in ImF(r) and hence the experimental temperature dependence can be also explained by such a rotation. From the other side, the simulations of $\chi_3(k)$ were performed under the fixed distances and bond-angles in Nb-O-Nb chain (non-rotated O_6-octahedron), but under the increased DW-parameter. The calculations revealed the F(r) temperature dependence in the third shell's r-range similar to that presented in Fig.2. For example the |F(r)| and Im F(r) of the $k^3\chi_3(k)$ term, calculated for Nb-O-Nb chain, which corresponds to the tetragonal phase of $KNbO_3$ under the two σ^2-parameters, differed from each other by 0.003 $Å^2$**,** are presented in Fig.3.

The results of simulations permit to conclude that the experimentally observed decrease of the third shell's peak in |F(r)| of B-atom's EXAFS in ABO_3 with the temperature can be explained both by the two effects, which are difficult to distinguish – the rotation of the O_6-octahedron and the increase of the DW-parameter. To distinguish these effects one can use the diffraction data on the DW-parameters in different temperature phases of crystal. The corresponding analysis of the temperature dependence in $KNbO_3$, obtained from the diffraction data (Darlington & Knight,1994) by the usually used prescription (Vedrinskii et al., 1986), gives the increase of the third shell's σ^2 value from 0.004 $Å^2$ in orthorhombic (T=300 K) to 0.007 $Å^2$ in tetragonal (T=543 K) phase i.e. by $\Delta\sigma^2$=0.003 $Å^2$. In Fig.3 the two theoretical curves |F(r)|, ImF(r) of $k^3\chi_3(k)$ calculated with the same σ^2 =0.004 $Å^2$ both for SS-process and MS-processes on the chain Nb-O-Nb, are compared with the corresponding two curves obtained with σ^2=0.007 $Å^2$. The comparison is performed under the fixed distances and angles in Nb-O-Nb chain i.e. under the XRD data on $\Delta\sigma^2$=0.003 $Å^2$ between the DW-parameters for the compared temperatures and in assumption of non-rotated O_6-octahedron. The comparison shows the ~ 1.5 times decrease of the max |F(r)| for the third shell's peak. As can be seen, this decrease appears to be quite similar to that, estimated from the experimental curve of Fig.1 between the corresponding two temperatures T=300 K and T=543 K. Therefore one can assume that the temperature increase of the DW-parameter only is sufficient to explain the temperature dependence of the third

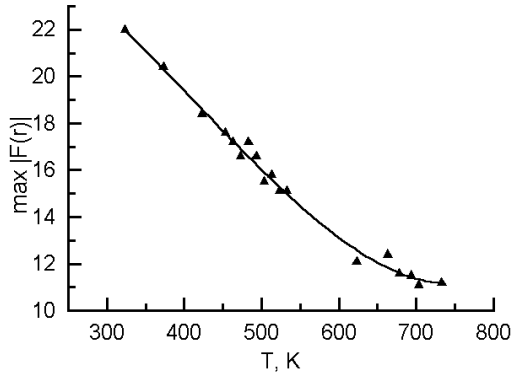

Fig.1. The temperature dependence of the third shell's peak value in |F(r)| of experimental $k^3\chi(k)$ in $KNbO_3$.

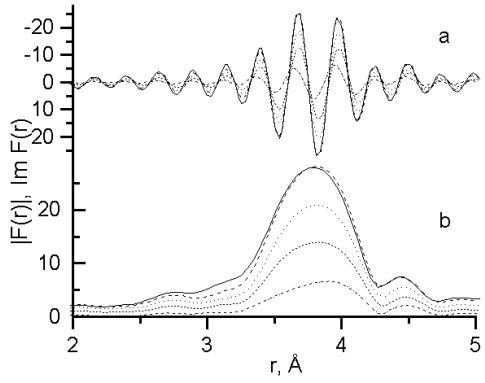

Fig.2. F(r) of the third shell term $k^3\chi_3(k)$ calculated for different d values: d=0 Å – solid, d=0.1 Å – dashed, d=0.2 Å – doted, d=0.3Å – short dashed and d=0.5 Å – dash-doted lines: (a) - Im F(r), (b) – |F(r)|.

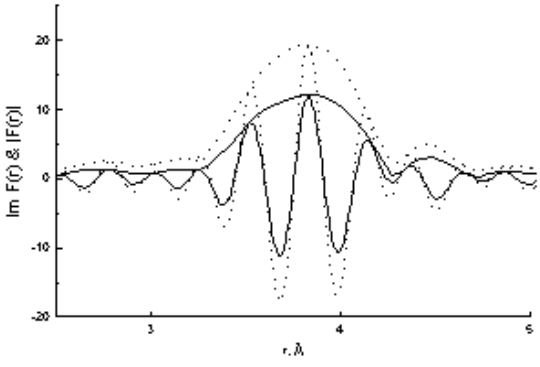

Fig.3. F(r) of the third shell term $k^3\chi_3(k)$ calculated for different σ^2: dashed curves–0.004 Å^2, solid curves–0.007 Å^2.

shell's peak value in |F(r)| of Nb EXAFS in $KNbO_3$ and the O_6-octahedron rotation doesn't occur in the high-temperature phases of this crystal.

To illustrate the sensitivity of F(r) in the third shell's r-region to the directions of B-atom's displacements in the neighboring cells of ABO_3, the theoretical Nb EXAFS for tetragonal $KNbO_3$ was simulated for the different models of Nb displacements along [211] direction, which was revealed from the analysis of the first shell term (Bugaev et al., 1999). The considered models for Nb displacements in the neighboring cells along [211] are: i) parallel shift ($\uparrow\uparrow$) of Nb-atoms; ii) anti parallel shift ($\uparrow\downarrow$); iii) the random distribution (RD) occur. Within these models, schematically illustrated in Fig.4, the interatomic distances and bond-angles in Nb-O-Nb chains, as well as the parameter Γ = 4 eV to account for the photoelectron inelastic losses, were fixed by the fitting results for the first shell (Bugaev et al., 1999) and the cell parameters for tetragonal phase. So the only variable parameter is the value of σ^2 for the third shell's term. The comparison of corresponding theoretical curves |F(r)| and ImF(r) with the experimental ones in Fig.5 shows that the best agreement is obtained for the ($\uparrow\uparrow$)-model under the distinguished differences in F(r) between the considered displacement models. Moreover, the applied fitting procedure gives the following values for the discrepancy factor (δ) between the experimental curves and the theoretical ones: $\delta_{\uparrow\uparrow}$ = 0.12; $\delta_{\uparrow\downarrow}$ = 0.51 and δ_{RD} = 0.35. The obtained result justifies the earlier results, obtained through the X-ray diffuse scattering (Comes et al., 1968) that the Nb-atoms in $KNbO_3$ are shifted in parallel directions from the centers of the neighboring O_6-octahedra.

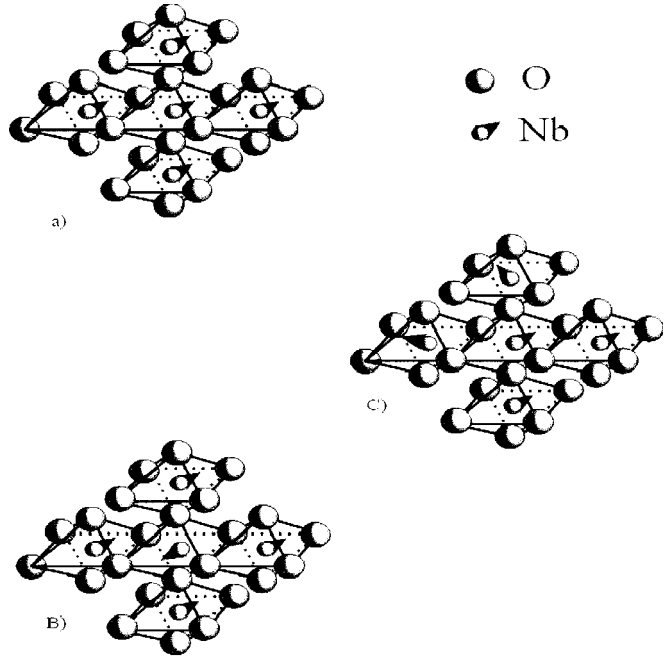

Fig.4. The illustration of the alternative models of Nb displacements: a) Nb-atoms are parallel shifted; b) Nb-atoms are anti parallel shifted; c) random distribution of Nb-atoms.

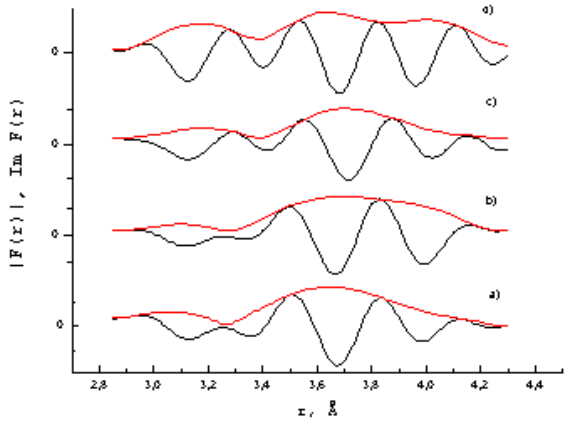

Fig.5. |F(r)|, ImF(r) of the experimental Nb EXAFS in $KNbO_3$ –(a) and of the third shell term $k^3\chi_3(k)$ calculated for alternative models of Nb displacements: (b)–Nb-atoms are parallel shifted; (c)–anti parallel; (d)–random distribution of Nb-atoms.

This work was supported by the grant of the program "Russian Universities. Fundamental Researches".

References

Bell M.I., Kim K.H. & Elam W.T. (1991). *Ferroelectrics*, **120**, 103-105.

Bugaev L., Shuvaeva V., Alekseenko I., Zhuchkov K. & Husson E. (1997). *J. Phys. (Paris)*, IV, **7**, C2-179-181.

Bugaev L., Shuvaeva V., Alekseenko I., Zhuchkov K., & Vedrinskii R. (1998) *Fiz. Tverd. Tela*, **40**, 1097-1101.

Bugaev L., Shuvaeva V., Zhuchkov K., Rusakova E., & Alekseenko I. (1999). *J Synch. Rad.*, **6**, 299-301.

Comes, R., Lambert, M. & Guinier, A. (1968). *Solid State Comm.*, **6,** 715.

Darlington C.N.V.& Knight K.S. (1994). *Phase Trans.* **52**, 261-275.

Petit P.E., Guyot F & Farges F. (1997). *J. Phys. (Paris)*, IV, **7**, C2-1065-1067.

Sicron N., Yacoby Y., Stern E.A. & Dogan F. (1997). *J. Phys. (Paris)*, IV, **7**, C2-1047-1049.

Vedrinskii R.V., Borovskii I.B., Kraizman V.L. & Sachenko V.P. (1986). *Uspekhi Fiz. Nauk*, **149**, 275-324.